Tribology International 82 (2015) 142–152

Contents lists available at ScienceDirect

Tribology International

journal homepage: www.elsevier.com/locate/triboint

Nonlinear dynamic behaviour of vertical and horizontal rotors in compliant liner tilting pad journal bearings: Some design considerations

Matthew Cha [a,b,*], Sergei Glavatskih [a,c]

[a] Machine Design, KTH Royal Institute of Technology, Stockholm, Sweden
[b] Waukesha Bearings, Rickmansworth, Hertfordshire, UK
[c] Mechanical Construction and Production, Ghent University, Ghent, Belgium

ARTICLE INFO

Article history:
Received 13 May 2014
Received in revised form
6 October 2014
Accepted 14 October 2014
Available online 22 October 2014

Keywords:
Compliant liner
Tilting pad journal bearings
Journal orbit
Bearing design parameters

ABSTRACT

Dynamic behaviour of vertical and horizontal rotors in journal bearings with line pivot pads is investigated. Two bearing designs are compared: one with white metal pads and another with compliant liner pads. The influence of elasticity of the liner on the journal orbits is investigated. Some practical aspects of the compliant liner pad design are discussed. Compliant bearing design parameters such as preload factor, pivot offset, radial clearance, viscoelasticity, and pad inclination to control the size of the journal orbit are considered.

1. Introduction

White metal is a traditional bearing liner material used to protect the shaft from damage. In this paper we study the effect of alternative liner materials on bearing response. Such materials are elastic polymers, and as previous studies showed [1–9], provide significant advantages over white metal. For example, a polytetrafluoroethylene (PTFE) liner reduces break-away friction during start-ups [1]. Inlet oil film temperature and maximum oil film pressure in a PTFE faced bearing are reduced as shown by the TEHD analysis in [2]. Experimental results also show that PTFE faced thrust bearings provide lower power loss and slightly higher shaft temperature compared to the white metal bearings [3]. It is explained in [4–6] how PTFE linings significantly extend steady state performance limits of the tilting pad thrust bearings.

In cylindrical journal bearings the oil film thickness and load carrying capacity are also improved while the maximum oil film pressure is reduced by up to 40% with the implementation of the compliant liner [7]. Once the bearing liner is changed from white metal to a polymer composite, the dynamic response of the journal bearing will be affected. This is due to the deformation of the polymer liner. Since deformation of polymer pads is larger than the white metal pads, the orbit size is also larger.

Viscoelastic characteristics of compliant liners in plain cylindrical journal bearings have been considered in [8]. The final journal equilibrium orbits in the viscoelastic case are located in between the orbits for white metal and purely elastic cases. Furthermore, dynamic behaviour of the compliant bearings can be controlled by changing properties of the liner material [8]. Tilting pads with compliant liners also show similar trends when supporting a horizontal rotor. Deformation of the compliant liner due to hydrodynamic pressure results in much thicker minimum oil film thickness in the pad mid-plane compared to white metal pads [9].

Since a positive influence of the compliant liner on the static operation of journal bearings has been established, the next step is to gain more insight into compliance effect on bearing dynamic response. Thus, this paper further explores the effect of liner compliance on the dynamic behaviour of tilting pad bearings supporting vertical and horizontal rotors. Dynamic behaviour of white metal and compliant liner bearings is compared considering different preload factors, pivot offsets, elasticity of the compliant liner material, and different pad inclinations. Some design modifications of the compliant bearing pads are also discussed.

2. Numerical model

The numerical approach developed is used to model tilting pad bearings and the effects of compliant liner on the shaft dynamic response. A rotor-bearing system with a rigid rotor supported by two identical tilting pad journal bearings is considered. The Reynolds

* Corresponding author at: Machine Design, KTH Royal Institute of Technology, Stockholm, Sweden. Tel.: +44 7474 838283.
E-mail address: match@kth.se (M. Cha).

http://dx.doi.org/10.1016/j.triboint.2014.10.011
0301-679X/

Nomenclature

C_b	bearing radial clearance (m)
C_p	pad radial clearance (m)
m	preload, $1-(C_b/C_p)$ $(-)$
F_x, F_y	fluid film forces (N)
L	bearing length (m)
M	rotor mass (kg)
R	journal radius (m)
W	static load (N)
d	pad thickness (m)
h	oil film thickness (m)
p	oil film pressure (Pa)
r	radial coordinate (m)
t	time (s)
x, y	coordinates of the journal centre (m)
$\ddot{x}, \ddot{y}$	acceleration of the journal centre (m/s^2)
z	axial coordinate (m)
δ_i	initial pad angle (rad)
δ_r	pad radial displacement (m)
μ	oil viscosity (Pa s)
θ	circumferential coordinate in a fixed frame (deg)
ω	angular speed of the journal (rad/s)
ξ	unbalance eccentricity (m)
ψ_i	pad pivot position (rad)

equation, equations of motion and pad deformation are solved simutaneously using a software package [10] to analyse bearing dynamics. Lubricant is considered to be Newtonian. Incompressible, isoviscous and laminar flow is assumed. In mild conditions, the temperature rise in the oil film is low. For example, in many hydropower units the maximum temperature in journal bearings is around 50–55 °C while the supply oil temperature is around 40 °C. Another example is bearings in subsea pumps. In the subsea applications, temperature rise in the bearing is less than 10 °C (60 °C inlet and 65 °C outlet, maximum temperature in the bearing is 67 °C). A practical reason for neglecting thermal effects is to reduce computational time to a manageable level (from 2–4 days to 3–5 h for one case).

2.1. Governing equations

Time-dependent Reynolds equation is written as follows:

$$\frac{1}{R^2}\frac{\partial}{\partial\theta}\left(\frac{h^3}{\mu}\frac{\partial p}{\partial\theta}\right)+\frac{\partial}{\partial z}\left(\frac{h^3}{\mu}\frac{\partial p}{\partial z}\right)=6\omega\frac{\partial h}{\partial\theta}+12\frac{\partial h}{\partial t} \quad (1)$$

The oil film thickness is given by

$$h=C_p-(C_p-C_b)\cos(\theta-\psi_i)-(R+d)\delta_i\ \sin(\theta-\psi_i) +x\ \cos(\theta)+y\ \sin(\theta)+\delta_r \quad (2)$$

The above equation takes into account pad tilt in the circumferential (sliding) direction only since the pads considered are with line pivots. Radial displacement term, δ_r, represents displacements due to both pad inclination and deformation. The motion of the journal centre of mass of the horizontal rotor is described by

$$M\ddot{x}=F_x+M\xi\omega^2\ \sin(\omega t)$$
$$M\ddot{y}=F_y+M\xi\omega^2\ \cos(\omega t)-W \quad (3)$$

For the vertical rotor, W equals zero. Deformations of the pad backing and compliant liner are calculated using a 6-by-6 elasticity matrix, which takes into account stresses and strains in the r, θ and z directions [10].

2.2. Boundary conditions

A symmetry boundary condition in the axial direction is imposed to reduce computational time. Pressure at the pad edges is set to ambient. A density–pressure cavitation model is implemented as shown in [8,9]. Saturation pressure is set to 20 kPa. A continuity condition is used at the interface between the pad backing and compliant liner for the displacements. At the pad-pivot interface, frictionless contact conditions are assumed. The pivot is assumed to be rigid with a radius of 5 mm.

2.3. Convergence and discretization

A grid of $5\times20\times7$ nodes in the r, θ, and z directions for each pad is used in the numerical model. There are two nodes in the radial direction in the compliant liner. A sensitivity study on the number of nodes in the compliant liner confirmed that two nodes across the compliant liner and a grid of $5\times20\times7$ nodes in the r, θ, and z directions are reasonable to accurately predict bearing dynamic behaviour. Additional nodes in the radial direction will dramatically increase the computational time. The final results are not noticeably affected by a further increase in the number of nodes in the pad backing and compliant liner. Since the pads are small, pad inertia does not affect the final results as shown in [9,11]. Convergence criteria for pressure and displacements are set to 10^{-7} Pa and 10^{-7} m. The convergence criterion of 10^{-9} was used to verify the accuracy of the final results. No visible differences were observed between the cases of 10^{-7} and 10^{-9}. In the simulations the static equilibrium position of the journal is obtained first. The journal is then subjected to an unbalance force.

2.4. Model verification

The numerical model is verified by comparing calculated results with [12]. Journal radius of 50 mm, bearing length of 70 mm and 4 pads were used. Results from the numerical model are in a good agreement with the published data [12].

3. Results

Fig. 1 shows the geometry of the tilting pad journal bearing used in this study. For the horizontal rotor configuration, a static load acts

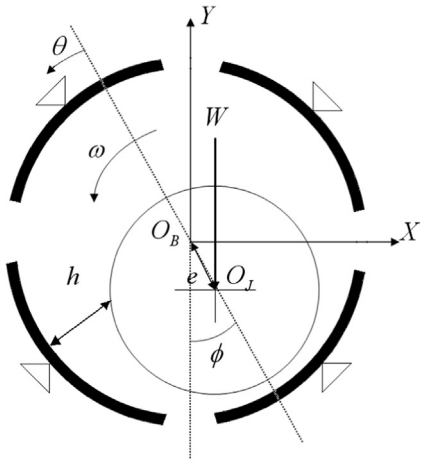

Fig. 1. Bearing geometry, load between pivots configuration.

downwards as shown in Fig. 1. For the vertical rotor configuration, there is no static load. Specification of the tilting pad journal bearing and liner properties, corresponding to PTFE, are given in Tables 1 and 2. Some bearing parameters will be varied in the course of the analysis to show their effect on the journal orbit. Such changes will be discussed in the corresponding section.

3.1. Rotor configuration

Journal orbits of the vertical and horizontal rotors are shown in Fig. 2. A non-dimensional coordinate system is used. An unbalance load of 5 kN is applied to the vertical rotor. A preload factor of 0.5 is used to compare white metal and compliant bearings. Fig. 2a presents the effect of the liner thickness on the journal orbit size, position and shape. Since there are four pads in the bearing, the journal orbit shape is a square with rounded corners. As the rotor approaches the pad, hydrodynamic pressure is built-up forcing the pad to tilt. Then the rotor is pushed away from the present pad to the next pad. For the white metal bearing, the maximum journal eccentricity is about 0.39 and the orbit is rotated 10 degrees in the sliding direction. A compliant liner of 1 mm in thickness increases the maximum journal eccentricity to 0.41 and rotates the orbit 15 degrees more in the sliding direction. For the 3 mm compliant liner, the maximum journal eccentricity becomes 0.48 while the angular shift increases to 34 degrees. The increase in the journal eccentricity and angular shift of the orbit are caused by the compliant liner deformation at the inlet part of the pad.

Fig. 2b presents journal orbits for the horizontal rotor configuration. The horizontal rotor is subjected to the unbalance load of 2.5 kN (50% W). The journal orbits are all lined up in the loading direction (between the pivots, see Fig. 1) because the pads can tilt. Maximum journal eccentricity in the white metal bearing is 0.3. For the 1 mm compliant liner, the maximum journal eccentricity is 0.32 and the orbit is slightly larger than for the white metal. Maximum journal eccentricity increases to 0.42 for the 3 mm liner and the lower part of the orbit shape is different compared to other two cases. It is flattened and stretched out in the sliding direction.

At 0.073 s (22.93 rad) the journal is located at the bottom of the orbit in the white metal bearing. For the 1 mm compliant liner, the bottom corner is moved to 0.0735 s (23.09 rad) position. And when the liner thickness is changed to 3 mm, the bottom corner is located at 0.0745 s (23.40 rad). Thus, 1 mm compliant liner provides a delay of 0.5 ms (0.16 rad) in time position compared to the white metal bearing. Compliant liner of 3 mm provides a delay of 1.5 ms (0.47 rad) in time position compared to the white metal bearing. Similar trends were observed in [9]. The delay is due to the compliant liner deformation that allows the journal to be pushed further in the radial direction. This trend can be controlled be the preload factor.

3.2. Preload effect

Preload m can be set in the range from zero to one. Lightly loaded bearings are purposely preloaded to stiffen the rotor-bearing system. The preload is changed by altering the pad radial clearance. Fig. 3a presents the dynamic behaviour of the vertical rotor in the compliant bearings (liner thickness 3 mm) with different preloads. The unbalance eccentricity is 100 μm, which corresponds to the unbalance load of 5 kN. As the pad radial clearance increases (preload also increases), the size of the journal orbit decreases. Preload factor of 0.9 shows a maximum journal eccentricity of 0.18. By increasing the preload factor from 0.5 to 0.9 the journal orbit is reduced by 65%. Fig. 3b compares maximum journal eccentricity for different preload factors and liner compliance. Journal orbit sizes in the white metal bearing with a preload factor of 0.5 and in the compliant bearings with preload factors of 0.57 and 0.69, liner thickness of 1 mm and 3 mm respectively, are comparable.

The influence of preload on the horizontal rotor behaviour is investigated with an unbalance eccentricity of 50 μm (50% W). Fig. 4a shows journal orbits for different preload factors, compliant liner thickness of 3 mm. The preload factor of 0.5 results in maximum journal eccentricity of 0.6 while the preload factor of 0.9 leads to maximum journal eccentricity of 0.18. Fig. 4b shows maximum journal eccentricities in white metal and compliant bearings as a function of preload factor. Journal orbit size in the white metal bearing with preload factor of 0.5 is comparable to the orbit size in the compliant bearings with preload factors of 0.57 and 0.68 for liner thickness of 1 mm and 3 mm respectively. If the compliant liner is thin (in our case 1 mm), the bearing behaves similar to the white metal bearing in terms of journal orbit size for preloads around 0.9. Results for different preload factors show that the compliant bearings need to be preloaded more to produce journal orbits and eccentricities comparable to the white metal bearings as shown in Figs. 3 and 4. It was not possible to obtain results for the compliant liner thickness of 3 mm with lower preload factors (0.1 and 0.25) due to the convergence issues.

3.3. Pivot offset effect

Fig. 5 shows journal orbits for two different pivot offsets for the vertical rotor configuration. Unbalance eccentricity of 100 μm is

Table 2
Compliant liner properties.

Young's modulus (E_P)	1.1×10^8 Pa
Poisson's ratio (ν_P)	0.46 [−]
Density (ρ_P)	2200 kg/m^3
Thickness (d_P)	1 and 3 mm

Table 1
Specification of the tilting pad journal bearing.

Journal radius (R)	0.05 m
Pad thickness (d)	0.015 m
Bearing length (L)	0.05 m
Bearing radial clearance (C_b)	1×10^{-4} m
Pad radial clearance (C_p)	2×10^{-4} m
Angular amplitude of pad	75°
Pivot positions	$\psi_1 = 45°$; $\psi_2 = 135°$; $\psi_3 = 225°$; $\psi_4 = 315°$
Pivot offset	50% or 65%
Lubricant viscosity (μ)	0.027 Pa s
Young's modulus (E)	2×10^{11} Pa
Poisson's ratio (ν)	0.33
Rotor speed (ω)	~314 rad/s (3000 rpm)
Gravitational load (W) (horizontal rotor configuration)	5000 N

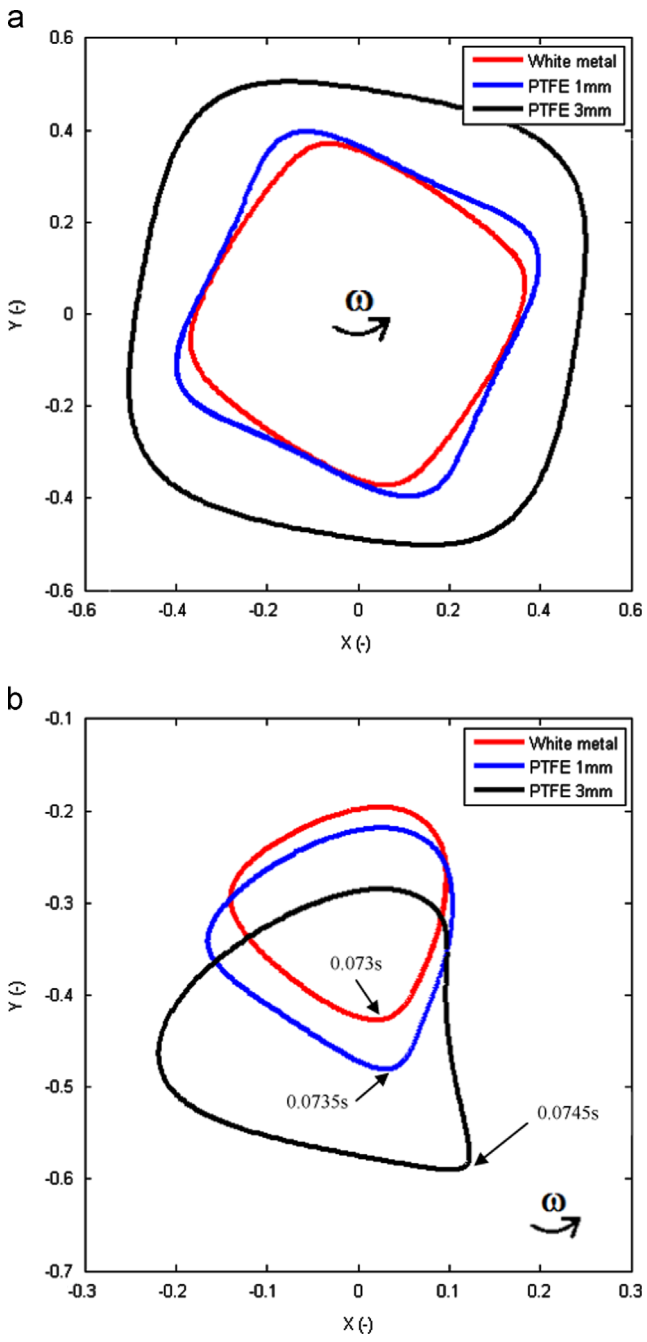

Fig. 2. Journal orbits: vertical (a) and horizontal (b) rotors.

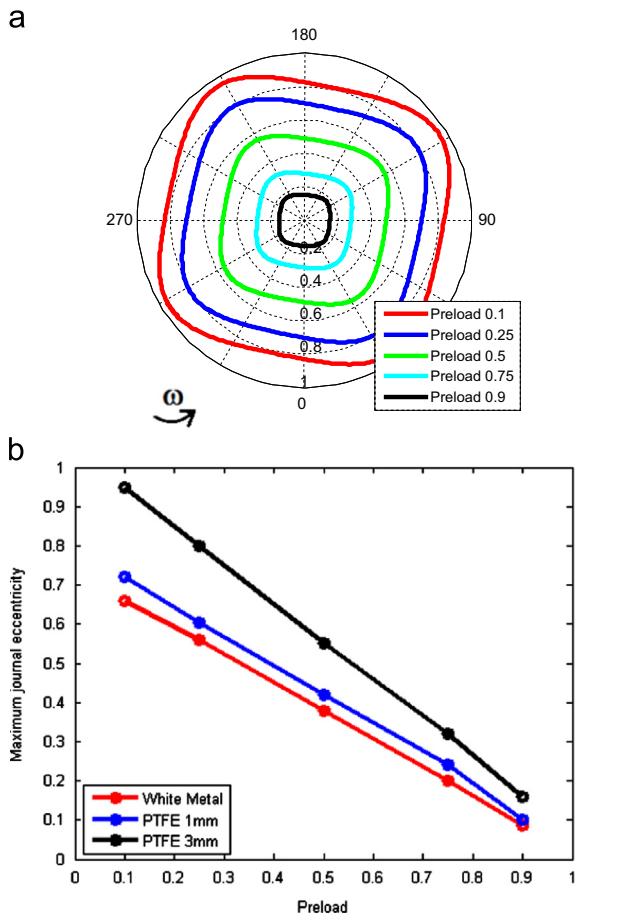

Fig. 3. Journal orbits of the vertical rotor: 3 mm liner thickness (a) and maximum journal eccentricity (b) for different preloads.

used. Compliant liner thickness of 3 mm with 50% offset pads is used as the reference case. Pivot offset of 65% results in a slightly smaller journal orbit size compared to the centrally pivoted pads. The journal orbit has also an angular shift of 15 degrees in the sliding direction due to the 65% pivot offset.

For a horizontal rotor configuration, pivot offset of 65% results in lower minimum journal eccentricity compared to the reference case. The journal orbit size is slightly larger for the pivot offset of 65%. From the bottom corner of the orbit, the time it takes for the rotor in the 50% offset pad bearing to reach the top and the left corners is 0.0745 s, (23.4 rad), 0.081 s (25.4 rad) and 0.089 s (28.0 rad) respectively. If the 65% pivot offset is used, the time it takes for the rotor to reach the bottom, top and left corners change to 0.076 s (23.9 rad), 0.083 s (26.1 rad) and 0.0885 s (27.8 rad) respectively. Precession speed of the rotor in 65% offset pad bearing results in slower response compared to the reference case, at the right corner.

The left corners of the orbit (Fig. 5b) have similar time positions. It takes 1.5 ms (0.47 rad) longer time for the rotor in the 65% pivot offset pads to reach the right corner. Then for the top corner, there is a 2 ms (0.63 rad) delay for the 65% pivot offset case. Higher pad inclinations lead to higher hydrodynamic pressure build up for the pads with 65% pivot offset compared to 50% pivot offset. This results in higher oil film reaction forces pushing the journal closer to the bearing centre. Maximum oil film pressure on 65% offset pad 1 occurs at 0.0751 s (23.6 rad), while for 50% offset pad 1, it occurs at 0.074 s (23.2 rad). The delay is caused by the further movement of the rotor to the right (Fig. 5b).

3.4. Radial clearance effect

The reference case (compliant liner thickness of 3 mm, pivot offset of 50%) is compared to the case of 30% smaller radial clearance. The preload factor is kept equal to 0.5 by decreasing both the pad and bearing radial clearances by 30% of the initial values. Fig. 6 shows that the decrease in the radial clearance results in about 10% smaller journal orbit size. The same phenomenon is observed if pivot offset is increased. A smaller radial clearance results in higher oil film pressure that pushes the journal closer to the bearing centre. Since pad compliance is unchanged, no angular shift of the journal orbit is observed. For the horizontal rotor, slightly smaller journal orbit size and lower journal eccentricity are obtained. A stretching effect of the bottom corner of the orbit is reduced for the 30% bearing radial clearance case.

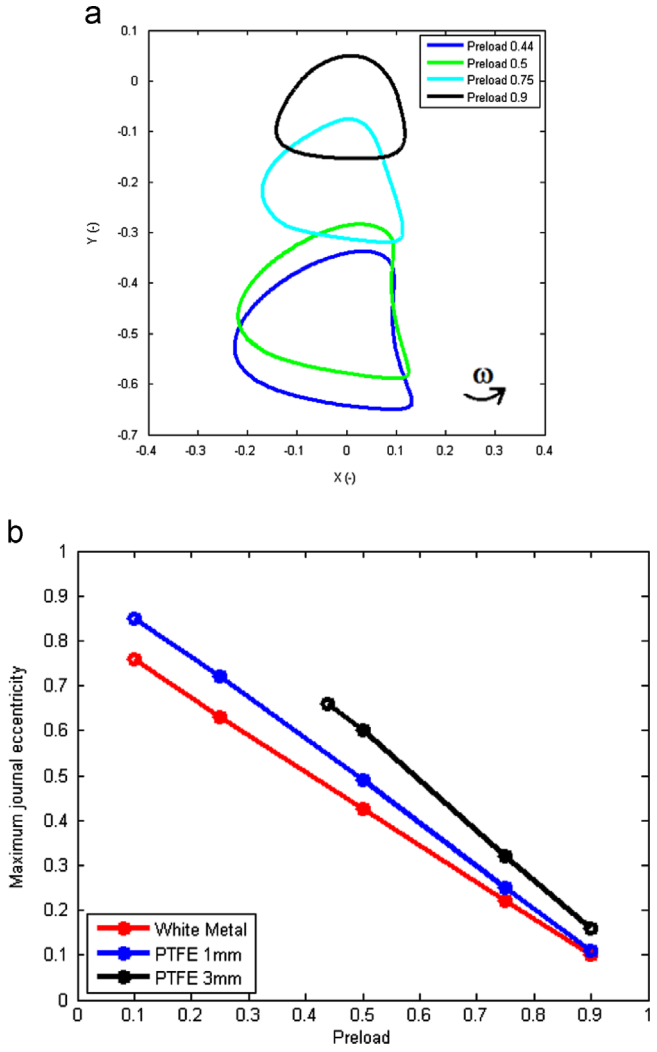

Fig. 4. Journal orbits of the horizontal rotor: 3 mm liner thickness (a) and maximum journal eccentricity (b) for different preloads.

3.5. Viscoelasticity

Polymers may not be purely elastic and exhibit some viscoelasticity. The viscoelastic properties of the PTFE layer (4 mm) were measured as described in [8] to fit a generalized Maxwell model. These properties are given in Table 3. An unbalance eccentricity of 50 μm (unbalance load of 2.5 kN) and 100 μm (unbalance load of 5 kN) is used for the horizontal rotor and the vertical rotor respectively to study the effect of viscoelastic properties on the journal orbit size, shape and position. Fig. 7a shows the vertical rotor orbits for the pure elastic and viscoelastic cases, compliant liner thickness of 3 mm. The white metal bearing gives the maximum journal eccentricity of 0.39. The purely elastic liner provides maximum journal eccentricity of 0.48. If viscoelastic properties are considered, maximum journal eccentricity slightly decreases from 0.48 (purely elastic case) to 0.45.

Measured relative stiffness coefficients of the PTFE layer, see Table 3, are multiplied by 50 to obtain material characteristics similar to polyetheretherketone (PEEK). Due to the lower compliance in the PEEK case, the journal orbit is shifted 15 degrees counter-clockwise approaching journal orbit in the white metal bearing for the vertical rotor case. A similar behaviour can be observed for the horizontal rotor, Fig. 7b. A slight decrease in journal orbit size is obtained for the PTFE case compared to the elastic case. PEEK produces a smaller journal orbit compared to the PTFE bearing since PEEK elasticity is 50 times higher. Furthermore,

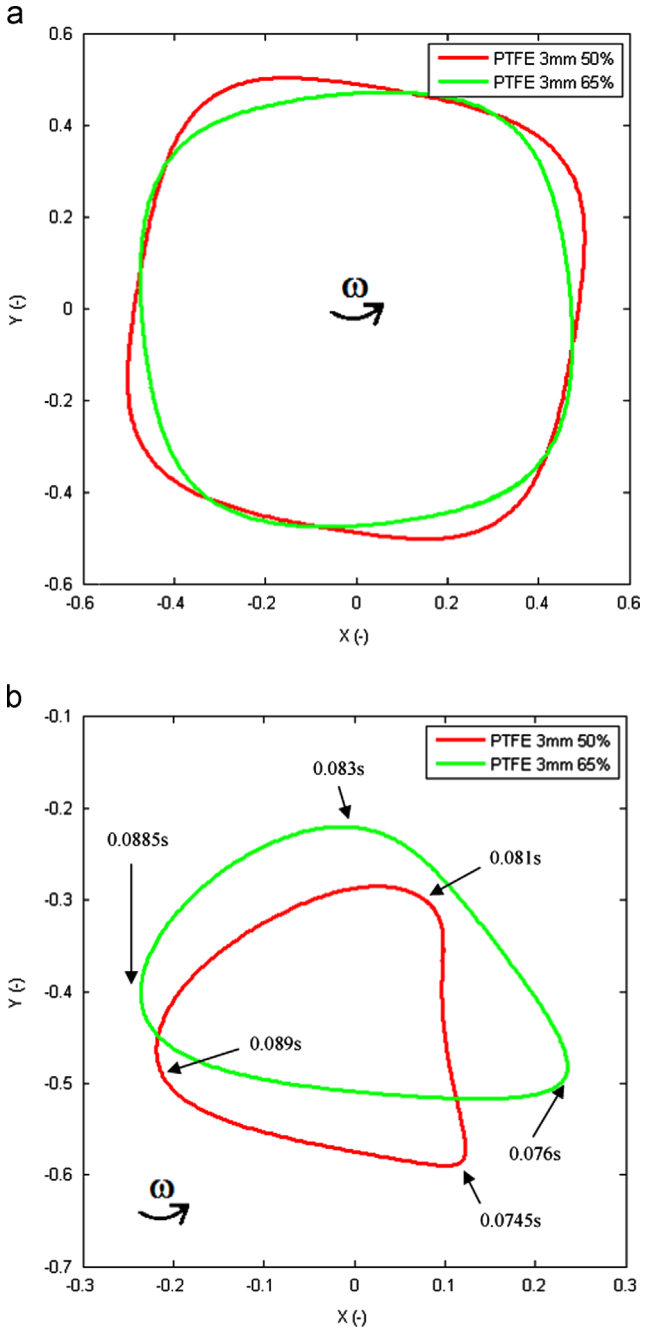

Fig. 5. Orbits of vertical (a) and horizontal (b) rotors; compliant liner thickness 3 mm.

PEEK 3 mm case shows rotor behaviour similar to the case with compliant liner pads (thickness of 1 mm) as shown in Fig. 2b.

3.6. Pad inclination

In 1994, Santos introduced a concept of controllable and adjustable fluid film bearings [13] by combining hydrodynamic and hydrostatic lubrication. By injecting pressurized oil in the bearing it is possible to modify and improve bearing dynamic characteristics (stiffness and damping). Such fluid film bearings can reduce vibration and instabilities (avoiding cross-coupling destabilizing effects) in the rotating machinery [14,15]. The principle of adjustable fluid film bearing is to change the hydrodynamic conditions during operation by continuously controlling and adjusting the pad tilt [15]. As shown in [15] the vibrations in the bearing can be suppressed

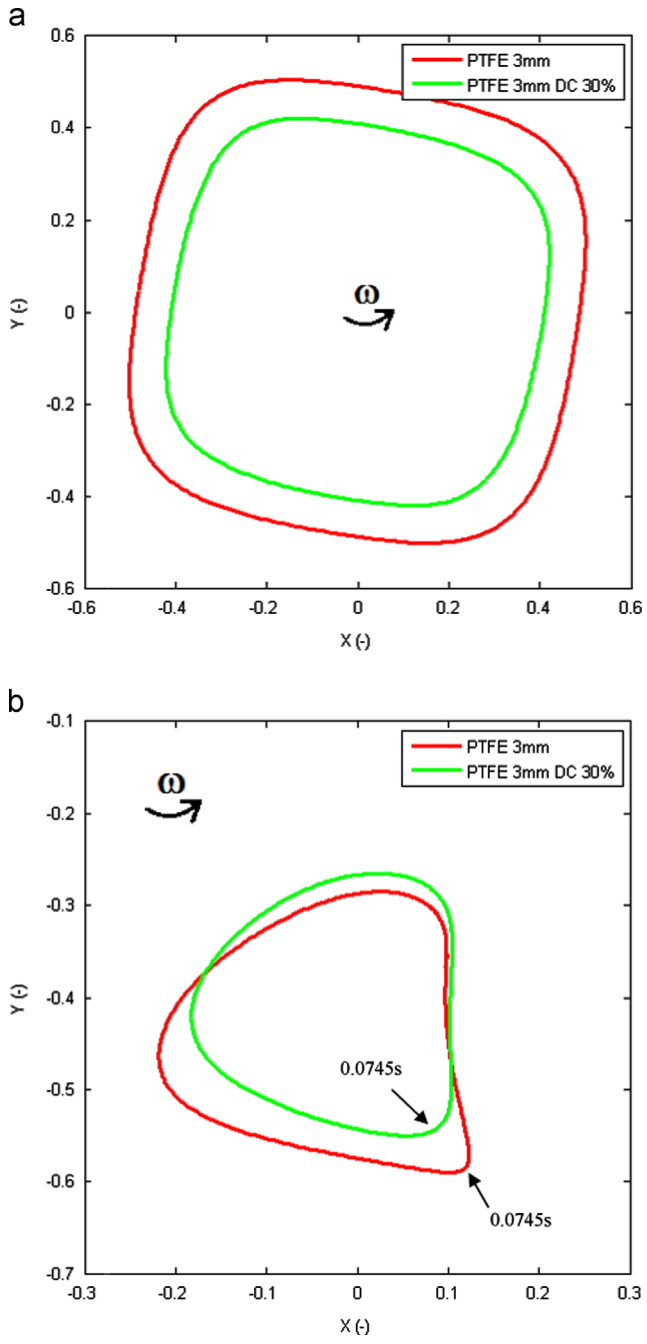

Fig. 6. Compliant liner thickness 3 mm, 50% pivot offset: vertical rotor (a) and horizontal rotor (b).

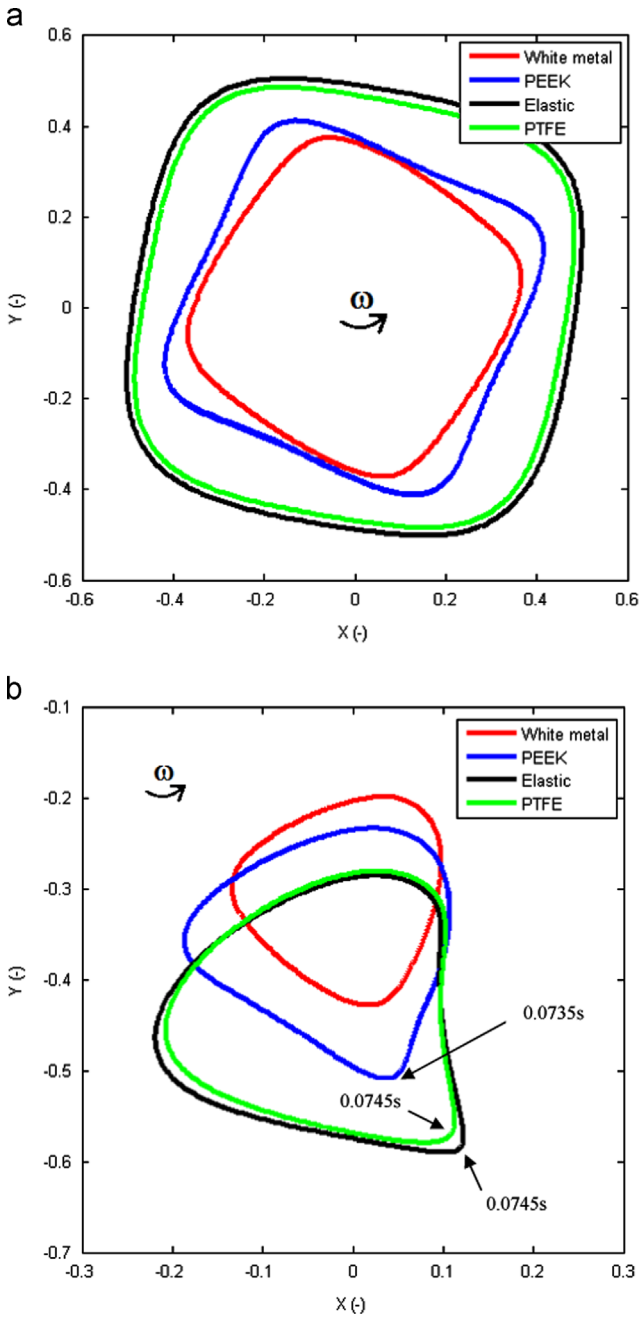

Fig. 7. Journal orbits for the compliant liner, thickness of 3 mm: vertical (a) and horizontal (b) rotors.

Table 3
Viscoelastic properties.

Branch	Relaxation time constant (s)	Relative stiffness
1	1	0.1272
2	6	0.1109
3	40	0.0033
4	251	0.0408
5	1,585	0.0233
6	10,000	0.0270

and the journal can be moved closer to the bearing centre by adjusting the bearing pads externally. We explore the idea of controlling journal orbits by fixing the compliant liner pads at different inclinations.

Fig. 8 shows journal orbits for the horizontal rotor configuration. At low pad inclination angle (0.01 degree) the final journal orbit is shifted in the sliding direction similar to journal behaviour in plain cylindrical journal bearings. The maximum journal eccentricity in this case is 0.62. The inclination angle of 0.1 degree gives larger journal orbit size than in the tilting pads. The maximum journal eccentricity in this case is approximately 0.46. Pad inclination angles greater than 0.1 degrees result in significantly reduced orbit size. When pads are fixed at 0.2 degree the maximum journal eccentricity is 0.3.

If the pads are free to tilt in the vertical rotor configuration (unbalance eccentricity of 100μm), the maximum journal eccentricity is about 0.48. If the pads are fixed at 0.01 degree, the maximum journal eccentricity is about 0.5. As the pad inclination angle increases, journal eccentricity decreases: pads fixed at 0.1 degree result in the journal eccentricity of 0.3; pads fixed at 0.2 degree result

in the journal eccentricity of 0.2. The orbit shape becomes circular at lower eccentricities because the journal does not move in between the pads. Pad inclination angle set to 0.05 degree gives a good agreement with the journal orbit size in the tilting pads.

3.7. Variable elasticity liner

A variation in tilting pad deformation as a function of time shows that the maximum deformation occurs at the front portion of the pads (from the leading edge to the pivot position). Thus, by stiffening the inlet half of the pads (circumferential EHS) as shown in Fig. 9a (blue colour for Young's modulus of 0.11 GPa and red colour for Young's modulus of 1.2 GPa), the journal orbit size can be decreased. For the vertical rotor configuration (Fig. 10a), the white metal bearing has the maximum journal eccentricity of 0.39 whereas the modified pad design has the maximum journal eccentricity of 0.42 (circumferential EHS). Due to the change in compliance of the bearing pads, the journal orbit is shifted 5 degrees in the sliding direction. For the horizontal rotor configuration (Fig. 10b), the trend is similar to the viscoelastic case (Fig. 7b). Liner modification reduces deformation as shown by the journal orbit size and time for the bottom corner of the journal orbit. Orbit corner time positions are exactly the same for the white metal and modified pads.

A variation in the elasticity can also be provided in the axial direction (axial ESH), Fig. 9b. The journal orbit size and shape are then similar to the orbit in the case of variable elasticity in the

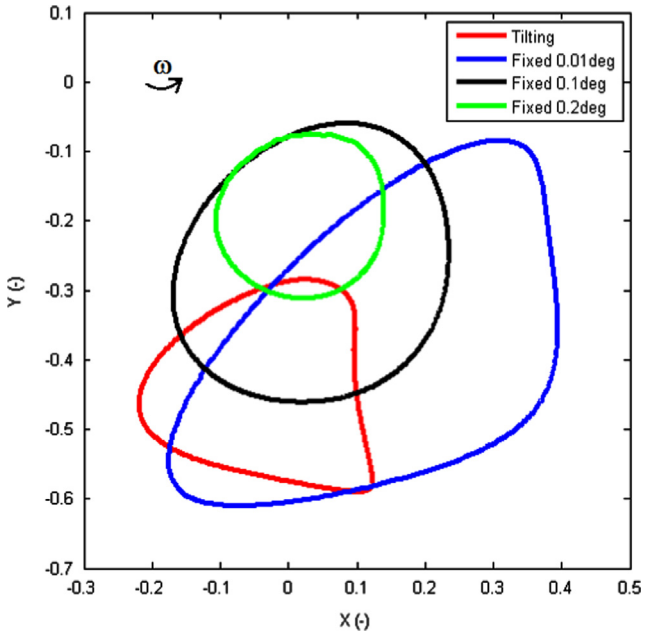

Fig. 8. Journal orbits, unbalance eccentricity 50 μm, compliant liner thickness 3 mm, horizontal rotor.

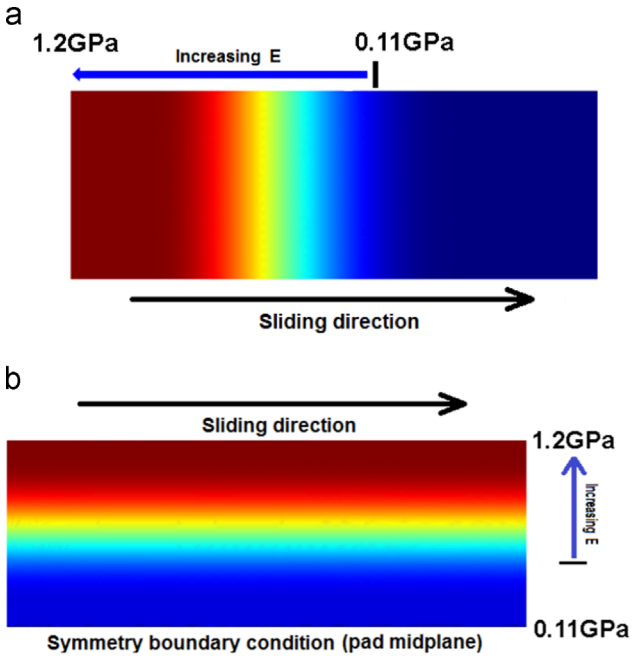

Fig. 9. Pad with variable elasticity of the liner, higher Young's modulus in the inlet part (a) and higher Young's modulus towards the pad edge in the axial direction (b). (For interpretation of the references to color in this figure legend, the reader is referred to the web version of this article.)

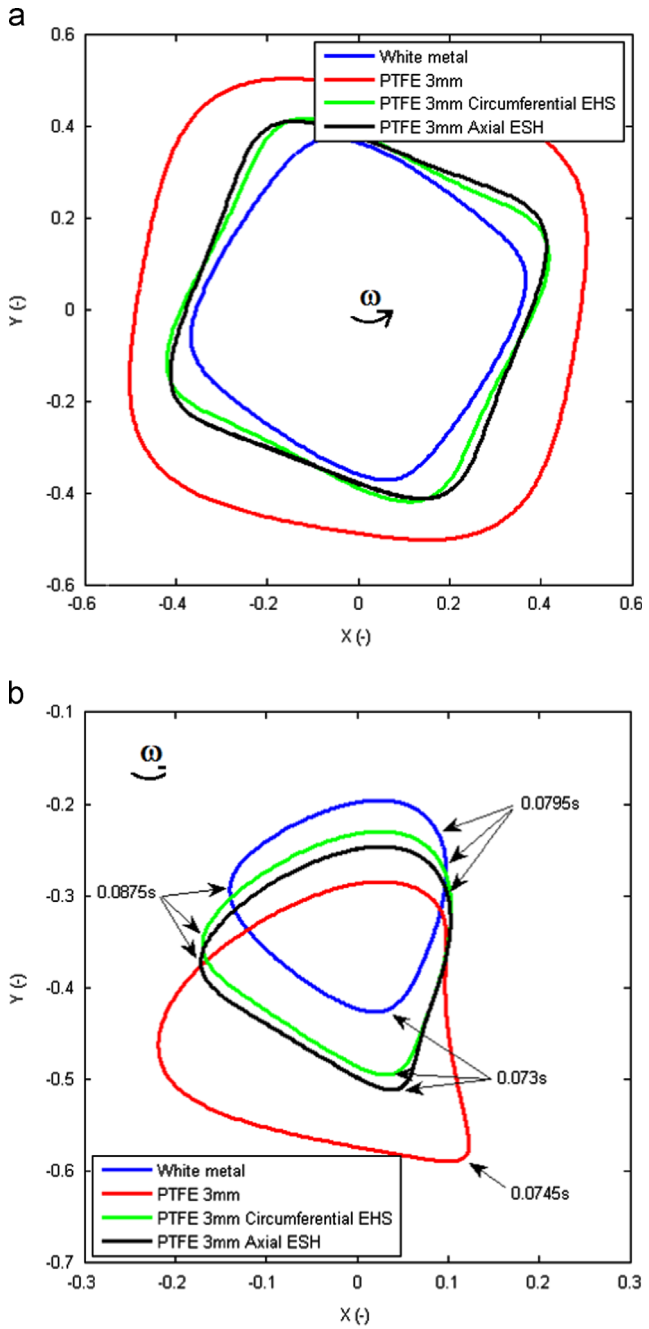

Fig. 10. Journal orbits, vertical rotor, $\xi = 100\ \mu m$ (a), and horizontal rotor, $\xi = 50\ \mu m$ (b).

axial direction. Maximum journal eccentricity becomes slightly higher, Fig. 10b.

Fig. 11 shows oil film pressure and oil film thickness profiles in the pad 4 midplane for the horizontal rotor configuration. In the 3 mm PTFE bearing, maximum oil film pressure is 6.2 MPa whereas in the white metal bearing, maximum oil film pressure is 7.3 MPa in the pad midplane. Lower maximum pressure and pressure gradients in the PTFE bearing are due to the compliance of the PTFE liner. Oil film profile in the 3 mm PTFE bearing is almost flat with a slight constriction at the outlet, 41 μm film thickness, similar in shape to the EHD contacts. The film profile in the white metal bearing has a minimum value of 35 μm in the maximum pressure region and a diverging part near the pad trailing edge.

With the variable elasticity in the circumferential direction (Fig. 9a, circumferential EHS), the pressure profile is significantly modified producing a maximum pressure of 7.9 MPa and a dip in the outlet pad of the pad. This dip corresponds to the increase in film thickness located after the minimum oil film thickness of 33 μm. The loss of pressure in the outlet part of the pad forces the maximum pressure to rise above maximum pressure for the white metal bearing. If elasticity modulus is increased in the sliding direction from the pivot area to the trailing edge (circumferential ESH) pressure raises even higher reaching 9 MPa. Oil film thickness profile is deformed in the inlet part (softer inlet part) and has a minimum value of 39 μm. A further increase in the maximum pressure to 9.2 MPa and a decrease in the minimum film to 28 μm can be achieved if the elasticity modulus is gradually decreased from the pad midplane to the pad side edges (axial EHS). This increase in pressure is due to the formation of the steep divergence in the outlet part of the pad.

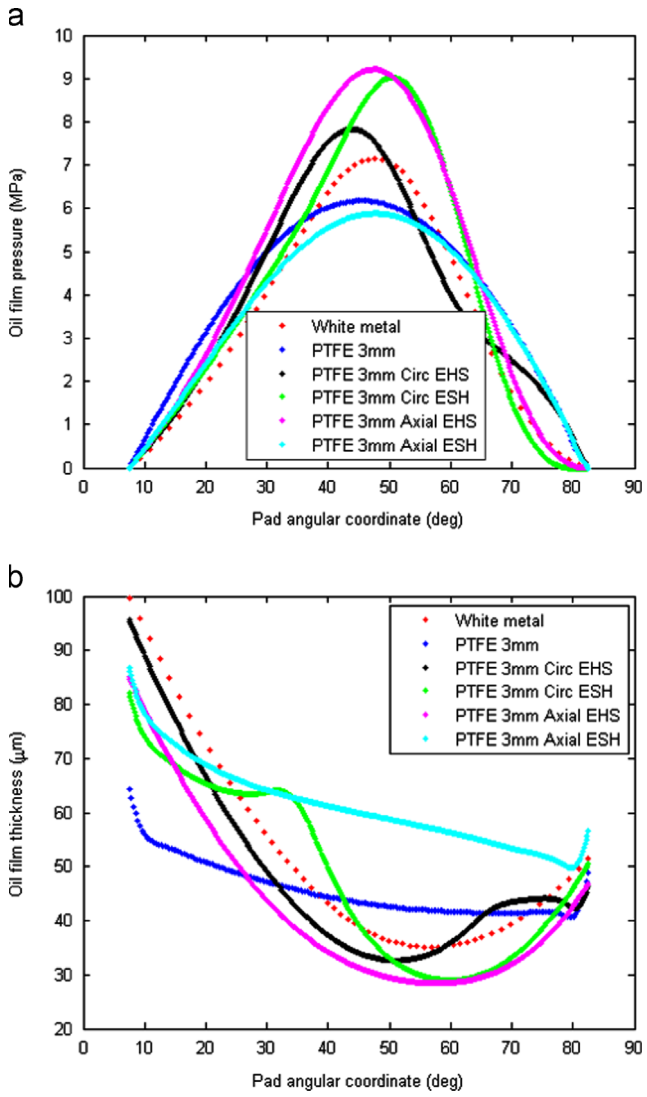

Fig. 11. Oil film pressure (a) and oil film thickness (b) for the pad 4, horizontal rotor; Circ EHS=circumferentially decreasing E modulus from the leading edge to the pivot area; Circ ESH=circumferentially increasing *E* modulus from the pivot area to the trailing edge; axial EHS=axially decreasing *E* modulus from the pad midplane to the pad edge; axial ESH=axially increasing *E* modulus from the pad midplane to the pad edge.

However, if elasticity gradually increases in the axial direction (Fig. 9b, axial ESH) from the pad midplane, oil film pressure in the midplane reduces to 5.9 MPa while minimum oil film thickness increases to 50 μm. Two pressure maxima of 6.6 MPa shifted towards the pad side edge in the axial direction are produced. This case gives also much smaller journal orbit compared to the PTFE 3 mm case.

In practice, it is difficult to vary Young's modulus in the liner. Therefore, the same results can be achieved by varying the liner thickness in the circumferential or axial directions.

3.8. Parameter interactions

In this section, interactions of different bearing design parameters are analysed. 9 parameter combinations are investigated for the vertical and horizontal rotor configurations. Unbalance load of 5 kN and 2.5 kN is used is used for the vertical and horizontal rotor respectively. Compliant liner thickness of 3 mm is chosen since it results in larger deformations of the liner which leads to the larger journal orbits. Figs. 12 and 13 show average power loss and average maximum journal eccentricity as a function of different parameter interactions for the vertical and horizontal rotor configurations. The parameters are: preload of 0.75, pad inclination of 0.15 degree, 30% decreased radial clearance, and 65% pivot offset.

Let us give an example on how much the journal orbits and the power loss in the bearing can be changed by combining different bearing design parameters. Adjusting the pivot offset from 50% to 65% decreases slightly power loss if compared with the compliant liner reference case (for the vertical and horizontal rotors). The compliant liner reference case (vertical rotor) gives an average maximum journal eccentricity of 0.48 and an average power loss of 993 W. Although decreasing bearing radial clearance increases the power loss, when two bearing parameters are combined (pivot offset and bearing radial clearance), it results in an average journal eccentricity of 0.39 and an average power loss of 1035 W. This shows that the average journal eccentricity can be reduced without a significant increase in the average power loss.

In the reference case of white metal bearing (50% pivot offset) the average power loss and average maximum journal eccentricity are approximately 1194 W and 0.39 for the vertical rotor configuration. If we use 65% pivot offset and preload of 0.75, the average power loss is reduced by 20% while the average maximum journal eccentricity becomes 0.3 (Fig. 12b). A decrease in power loss is due to the thicker oil film thickness for compliant liner pads compared to the white metal pads. Similar trends in power loss and journal eccentricity are obtained for the horizontal rotor configuration.

4. Conclusions

The dynamic behaviour of the vertical and horizontal rigid rotors in compliant tilting pad journal bearings was investigated for the line pivot pads. Compliant liner results in larger journal orbits, lower maximum oil film pressure and increased minimum oil film thickness in the bearing midplane compared to white metal liner.

- Deformation of the compliant liner does not change the vertical rotor orbit shape but provides an angular shift in the orbit

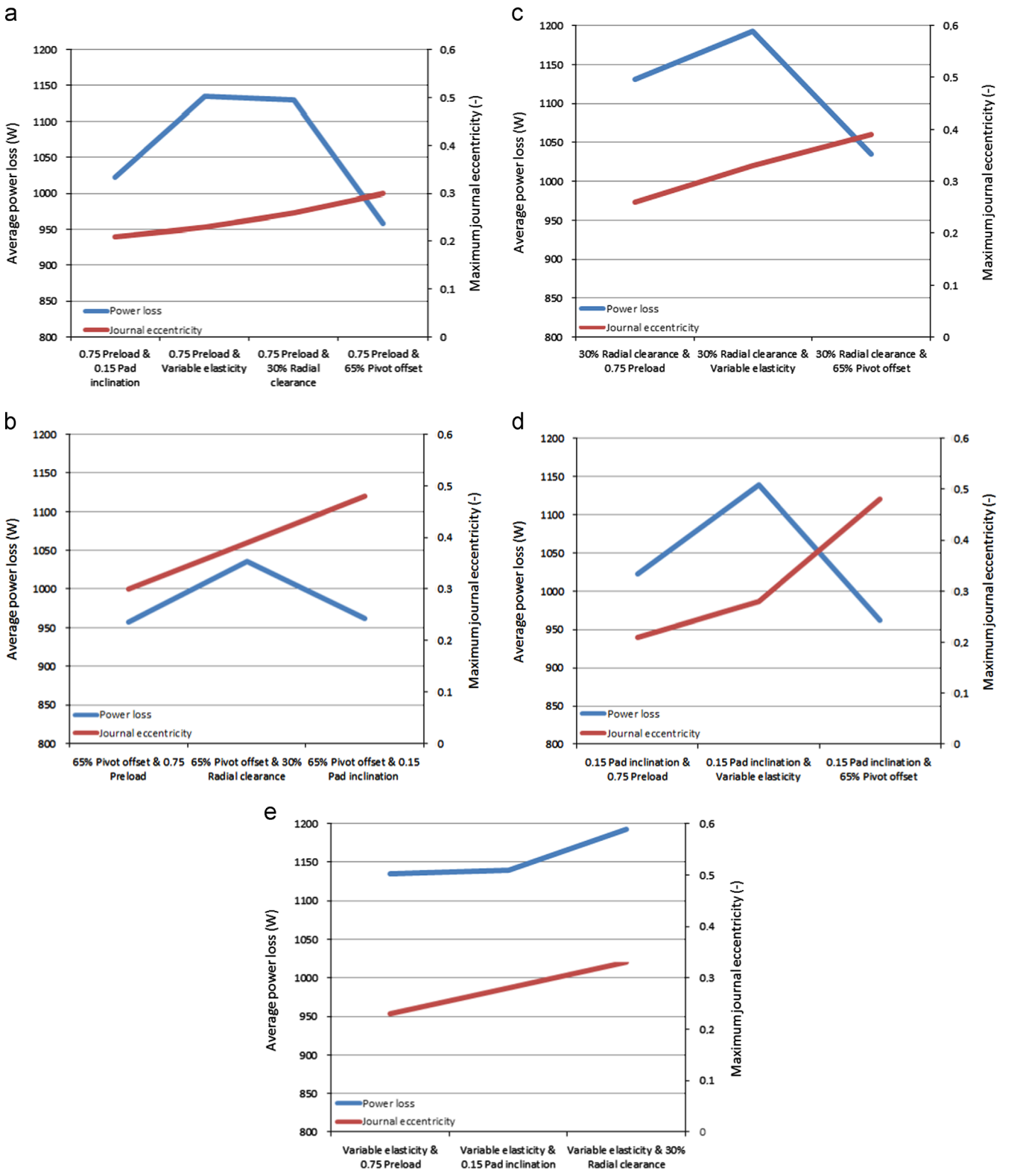

Fig. 12. Power loss and journal eccentricity as a function of parameter interaction for vertical rotor.

orientation in the sliding direction. The shape of the horizontal rotor orbit is significantly affected by the compliant liner thickness. Compared to the elastic liner, viscoelasticity does not change the orbit shape and orientation but reduces the maximum eccentricity.

- Compliant bearings should be preloaded more to provide journal orbits similar to the white metal bearings. For example, in our case for the liner thickness of 1 mm, compliant bearing should have 14% higher preload to provide journal orbits comparable to the orbits in the white metal bearing with preload 0.5.
- A pad liner that is stiffer at the pad side edges compared to the uniform elasticity liner provides similar maximum oil film pressure (but with two peaks) and increased minimum oil film thickness (in the pad midplane). It also provides smaller journal orbit size compared to 3 mm uniform liner.

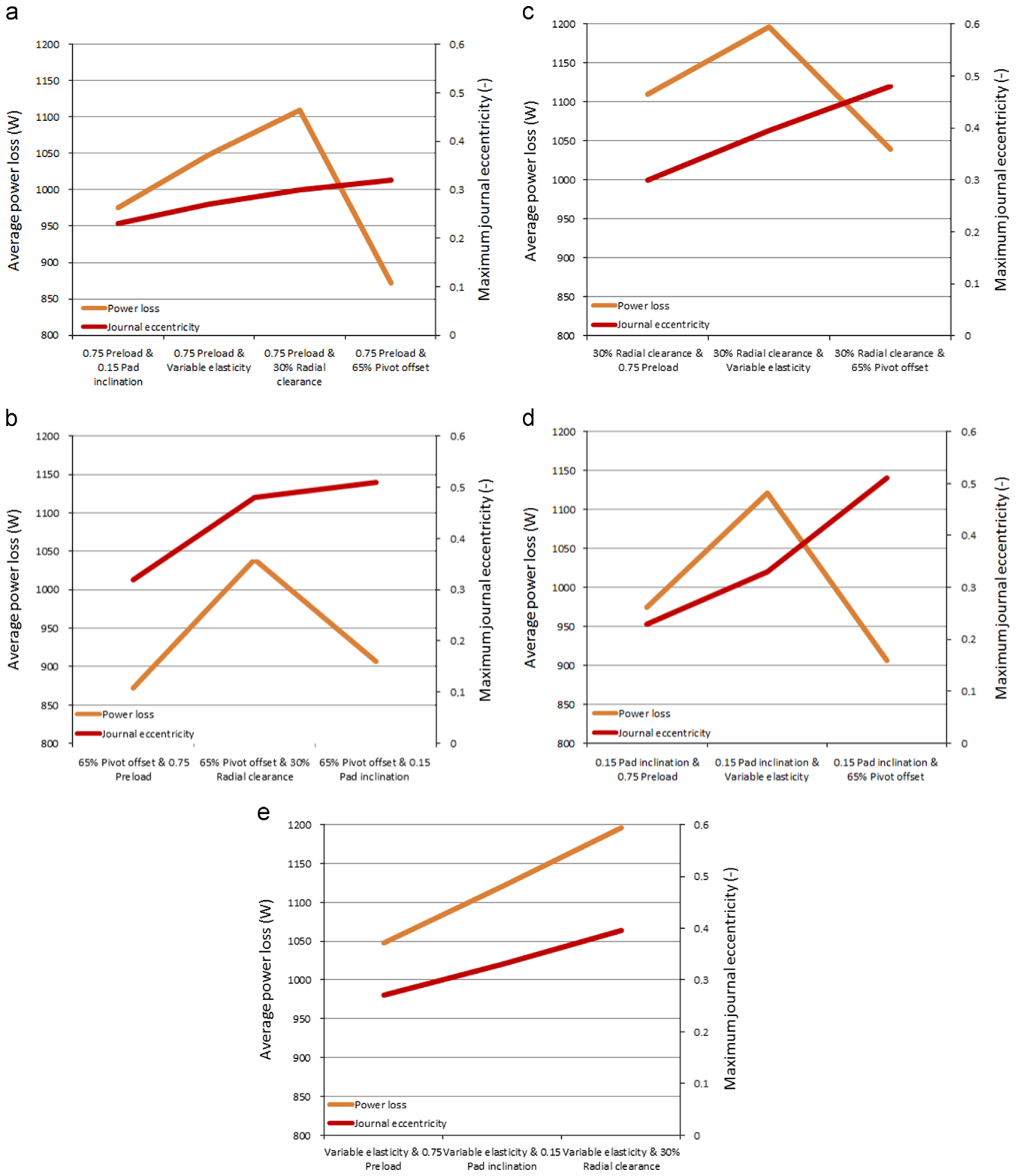

Fig. 13. c) Power loss and journal eccentricity as a function of parameter interaction for horizontal rotor.

- A thicker oil film thickness over the pad in the compliant bearing explains slightly lower power loss than in the white metal bearing. Power loss can be further decreased by selecting an appropriate combination of such design parameter as pivot offset and preload. It is also an efficient way to constrain the rotor movement in the bearing.
- The rotor orbit in the compliant bearing can be efficiently controlled by changing pad inclination angles.

Acknowledgements

The research is supported by the Swedish Hydropower Centre (SVC). SVC has been established by the Swedish Energy Agency, Elforsk and Svenska Kraftnät in partnership with academic institutions.

References

[1] Golchin A, Simmons GF, Glavatskih SB. Break-away friction of PTFE materials in lubricated conditions. Tribol Int 2012;48:54–62.

[2] Glavatskih SB, Fillon M. TEHD analysis of thrust bearings with PTFE-faced pads. J Tribol 2006;128(1):49–58.
[3] Glavatskih SB. Evaluating thermal performance of a PTFE-faced tilting pad thrust bearing. J Tribol 2003;125(2):319–24.
[4] Markin D, McCarthy D, Glavatskih S. A FEM approach to simulation of tilting pad thrust bearing assemblies. Tribol Int 2003;36:807–14.
[5] Fillon M, Glavatskih S. PTFE-faced center pivot thrust pad bearings: factors affecting TEHD performance. Tribol Int 2008;41(12):1219–25.
[6] Glavatskih S, Wasilczuk M, Fillon M. Unique performance aspects of PTFE-lined thrust bearings. HRW J 2005;13(6):32–7.
[7] Kuznetsov E, Glavatskih S, Fillon M. THD analysis of compliant journal bearing considering liner deformation. Tribol Int 2011;44(12):1629–41.
[8] Cha M, Kuznetsov E, Glavatskih S. A comparative linear and nonlinear dynamic analysis of compliant cylindrical journal bearings. Mech Mach Theory 2013;64:82–92.
[9] Cha M, Isaksson P, Glavatskih S. Influence of pad compliance on nonlinear dynamic characteristics of tilting pad journal bearings. Tribol Int 2013;57:46–56.
[10] Comsol Multiphysics User's Guide, Version 3.5a; 2008.
[11] Okabe EP, Cavalca KL. Rotordynamic analysis of systems with a non-linear model of tilting pad journal bearings including turbulence effects. Nonlinear Dyn 2009;57(4):481–95.
[12] Fillon M, Desbordes H, Frene J. A global approach of thermal effects including pad deformations in tilting-pad journal bearings submitted to unbalance load. J Tribol 1996;118(1):169–74.
[13] Santos IF. Design and evaluation of two types of active tilting-pad bearings. In: IUTAM symposium on active control of vibration, Bath, UK; 1994. p. 79–87.
[14] Santos IF. Trends in controllable oil film bearings. In: IUTAM symposium on emerging trends in rotor dynamics; 2011. vol. 1011, p. 185–199.
[15] Martin JK. A mathematical model and numerical solution technique for a novel adjustable hydrodynamic bearing. Int J Numer Methods Fluids 1999;30(7):845–64.